

# Study of The Drying on The Pore Network in order to Comparison of the Phase Distribution between Measured and Simulated Results

*Tran Quoc Tiep, Ta Hong Duc\**

*Hanoi University of Science and Technology – No. 1, Dai Co Viet Str., Hai Ba Trung, Ha Noi, Viet Nam*

*Received: Demcember 20, 2017; Accepted: May 25, 2018*

## **Abstract**

*Non-isothermal drying processes are empirical studied on the pore network at the different temperature gradients. Their results have been compared with a corresponding mathematical model. To conduct the empirical experiment, a pore network with 50x50 pores, are created by electron lithography method. The temperature distribution from the top to the bottom of the network is determined by an infrared camera and then these results are adopted in the mathematical model algorithm. During the drying process, the series of images showing the phase change in network is observed and recorded, which will be processed with an algorithm built in MATLAB. From that, we find out the change of network saturation, drying rate and the increase in the number of clusters and in the size of the main cluster in network. The phase distribution in the experiment is consistent with the simulation results at different temperature gradients.*

Keywords: Drying model, Non-isothermal, pore network

## **1. Introduction**

In order to model the drying process, continuous model has become a common tool for provide more understanding of drying at the macro level. However, the continuous model and the experimental results at the macro level are unable to given the phenomena at the micro level (capillary scale) [1].

The liquid evaporates at the phase boundary, then vapor diffuses into the gas phase in the direction from where has high pressure to where has low pressure. In the pores, liquid moves from large pores to smaller pores because of capillary pressure difference. These processes occurring at the micro level could be described by a discrete mathematical (pore network) model. This pore network model represents the structure of porous materials with pores and throats. Through which, we have the ability to describe the effects of physical quantities such as: capillary, temperature, viscosity and gravity, which affect the distribution of the liquid in the network.

The investigation of the drying process on porous medium with pore network has conducted. Yiotis and Tsimpanogiannis simulated the isothermal drying process on a 2D network and presented the phase distribution in the presence and absence of the gravity [2]. Laurindo and Prat investigated the effect of gravitation on the drying potential and phase distribution under isothermal conditions with the absence of viscosity [3, 4]. Mathematical modeling of

Plourde and Prat also extended the heat transfer calculations. They have find out the influence of temperature gradients on phase distribution of the gas and liquid [5]. Whereas Huinink focused on the influence of temperature on the drying process [6]. Surasani and Metzger investigated the heat transfer in mono- and bimodal structures during the drying process in convection drying and contact drying [1,7]. However, the statements of all these authors just limited to the simulation model but not yet conducting empirical research in order to verify.

Therefore in this report, the process of drying in the pore network under non-isothermal and isothermal conditions are conducted and implemented in the mathematical model. Then the results of experiments and simulations are compared and discussed.

## **2. Materials and methods**

### **2.1. Experimental setup**

The pore network with the size of 50x50 pores used in the experiment ist made from a thin layer of quartz (SiO<sub>2</sub>), on it the pores and throats are created by electron lithography. The length of the throats is 1000 μm. The width of the throats is normallz distributed with the mean of 150 μm and the standard deviation of 15 μm. Under the quartz layer a Silicium surface is sealed to create a 3-sides-closed network. At the top side of the network the water can evaporate and escape into the air. (Fig.1 and 2).

\*Corresponding author: Tel.: (+84) 916938659  
Email: duc.tahong@hust.edu.vn

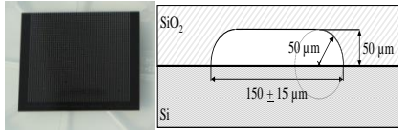


**Fig. 1 & 2.** Pore network Si - SiO<sub>2</sub>, Cross section of the throat

An aluminium plate placed under the network will create temperature gradients. Two water flows pumped from the thermostats flow through this metal plate. The adjustment of water temperature in the thermostats will allow the creation of different temperature gradients. In addition, an air flow (at room temperature) is blown through the network opened side to sweep away moisture evaporating from the inside of the network.

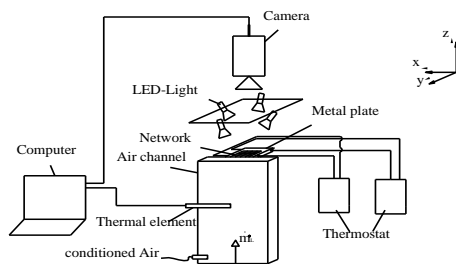


**Fig. 3.** The experiment system

The drying process is recorded by a digital camera Panasonic AG-HVX 200E, which is controlled by the Software IC- Capture (Version 2.2.174.793). The data of temperature and humidity in the air is collected by the software Daisy – Lab (Version 10.00.01)

**2.1.1. Temperature measurement**

During the experiment, heat is transferred from the metal plate into the network. The temperature profiles between the heat flows are not linear from the open side to the bottom side of the network. To have a view of this temperature field on the network, we used an infrared camera IR 8300, Infratec (with Spectral range: 2.0 μm – 5.7 μm, Temperature resolution at 30 °C: 0,025K, Temperature measuring range: -40°C - 1200°C) to conduct a direct measurement on the network. The temperature data is processed by IRBIS 3 Professional, which can perform the temperature profile on the network easily. In the temperature measurement using infrared camera, the emissivity of the object plays an determining roll. Because of the emissivity of the quartz surface is approximately equal to 1, thus the temperature measurements on the surface have very high accuracy. Furthermore, the silicium plate placed under the network is very thin, about 100 μm, so the thermal conductivity from

Aluminum metal plate into the pores can be considered without loss.

In each measurement, a correspondent thermal diagram is created and saved. Each pixel in this diagram represents a corresponding temperature value. Then, all temperature values will be collected and stored into a matrix (Fig.4)

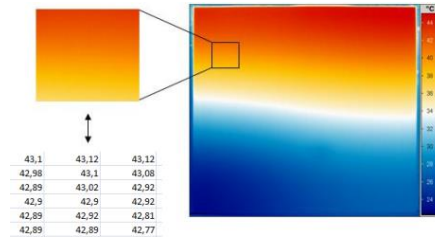


**Fig. 4.** The thermal diagram of the pore network

**2.1.2. Image processing**

Initially, to determine the saturation of the network, the images taken in the experiment (Fig.5.1) are processed with an algorithm built in Matlab. In which, each RGB image is converted to a binary image with a determined gray value. Then, algorithm determines all the black pixels (with value 1) of each pore and throat, and makes decision whether these pores and throats are saturated (full), partially saturated (partially full) or unsaturated (empty). (Fig.5.2)

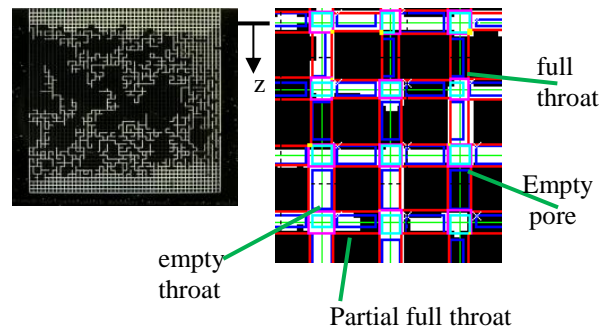


**Fig. 5.1** (left) RGB image and **5.2** (right) Binary image, determining the saturation

The percentage of the black pixels in total pixel of a pore or throat will determine its saturation:

$$S = \frac{P_{is}}{P_i} \tag{1}$$

P<sub>is</sub> is the number of black pixels and P<sub>i</sub> is the total number of pixels in a pore or throat. Saturation of the whole network is calculated according to this formular:

$$S_{Network} = \frac{\sum_{i=1}^{N_T} S_{ij} \cdot V_{ij} + \sum_{i=1}^{N_P} S_i \cdot V_i}{\sum_{i=1}^{N_T} V_{ij} + \sum_{i=1}^{N_P} V_i} \quad (2)$$

$S_{ij}$  and  $V_{ij}$ , are respectively saturation and volume of throat  $ij$ ;  $S_i$  and  $V_i$ , are respectively saturation and volume of pore  $i$ ;  $N_T$  is the number of throat and  $N_P$  is the number of pore in the network.

Drying rate describes the change of network saturation over time ( $t$ ) and is calculated as:

$$\frac{dS}{dt}(\bar{S}_i) = \frac{S_i - S_{i+1}}{t_{i+1} - t_i} \quad (3)$$

with  $\bar{S}_i$  is the average saturation between two consecutive times during the drying process:

$$\bar{S}_i = \frac{S_i + S_{i+1}}{2} \quad (4)$$

### 2.2 Pore network modeling

In the mathematical model, which is used to describe the drying process, the size of the network and the experimental conditions are applied. Temperature field in experiment is adopted into the model and kept constant during the whole drying process. Further more condensation phenomena also be considered in this model. However heat transfer is not calculated. Figure 6 shows the algorithm of the model.

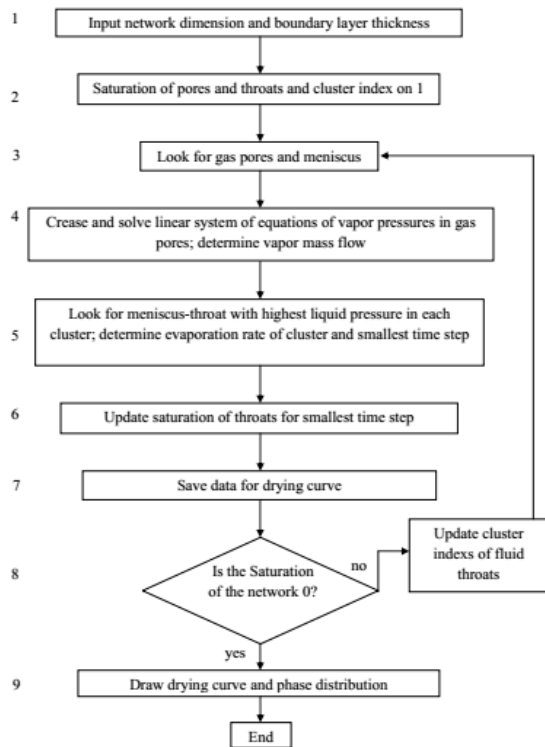


Fig. 6. The diagram of algorithm simulating the drying process

### 3. Results and discussion

Comparison of the phase distribution in the experiment and the simulation shows information whether the results have a qualitative agreement or not. That means, with the existing model the behaviors during the drying process can be described exactly depending on the direction and magnitude of the temperature gradient or not. The result images present the phase distribution in experiment and simulation at the same network saturation. Different from the experiment, in the simulation the partially-saturated pores and throats are also considered. In the simulated phase distribution, pores and throats with saturation  $S = 1$  are represented in black, with saturation  $S = 0$  in white. Pores and throats, where the condensation takes place, are shown in blue and where the evaporation takes place in red.

a)  $dT/dz > 0$

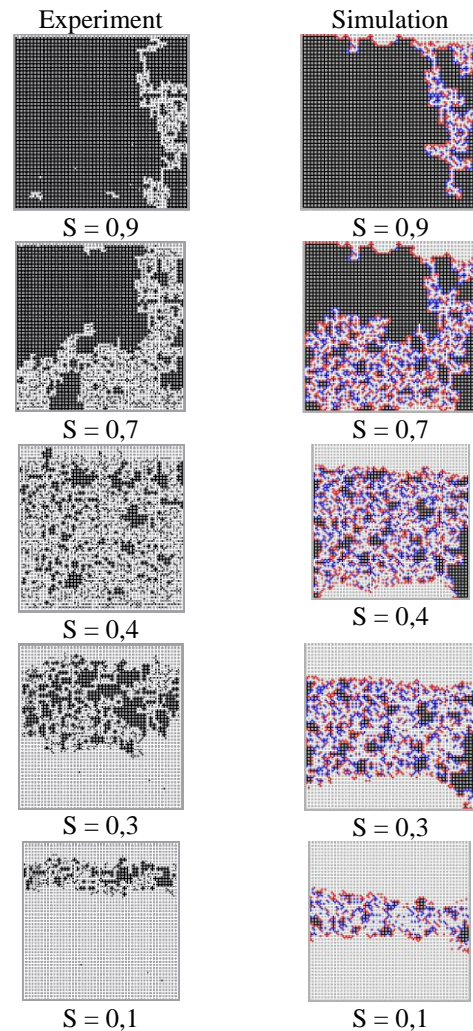
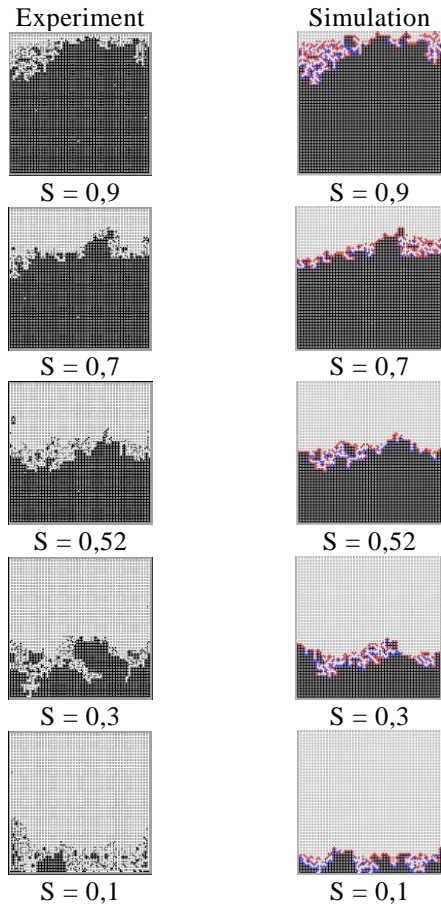


Fig.7. Phase distribution of the experiment and simulation for case  $T_0 = 27^\circ\text{C}$ ,  $T_L = 50^\circ\text{C}$



**Fig.8.** Phase distribution of the experiment and simulation for case  $T_0=75^\circ\text{C}$ ,  $T_L=52^\circ\text{C}$

The phase distribution observed in experiment and simulation (Fig.7) are agreed qualitative with the results in the reference [6]. First, a "single branch" enters in the network ( $S=0,9$ ). After the air reaches the bottom of the network (breakthrough of gas), then drying front move to inside of the network. Evaporation takes place mostly at the opened side, and does not occur in the network inside (because here there is saturation vapor pressure). At the below, the pores with higher liquid pressure will push the water up to the network surface. When the drying front enters inside the network, at the same time, the invasion into the liquid phase occurs. At the saturation  $S=0,4$ , in experiment, the whole liquid phase is divided into small clusters. Cluster in the highest position (at  $S=0,4$ ) is still linked to the the network surface. In the simulation, at the same time, the clusters are larger and the drying front locates deeper inside the network. Finally, in both experiment and simulation the second drying front appears, while the first drying front does not continue to go inside the network ( $S=0,3$  and  $S=0,1$ ). This phenomenon is very similar to the results of Huinink [6]. At the end of the drying process (with  $S=0,1$ ), the liquid in the experiment is near the network surface, and in simulation it locates deeper inside the network.

b)  $dT/dz < 0$

Figure 8 compares the phase distribution in experiment and simulation for the case  $dT/dz < 0$ . These phase distributions are accurate until the saturation  $S=0,52$ . At this moment in the experiment, there are more clusters separated from the drying front. Do these clusters exist alone or are they linked to each other through liquid films? This question should be answered in next experiments. Moreover, a same phase distribution like these results was found in results of Prat [8]. A part of the main cluster has contact to the completely dry area, and water only evaporates from the clusters within the drying front as well as from the main cluster [8].

At the saturation  $S=0,3$ , the air in the experiment reach the bottom of the network while drying front in the simulation is still stable. We can see that the distributions are very different: in the experiment, the drying front continues to be invaded by the gas phase and lead to increasing the number of clusters ( $S=0,1$ ) whereas in the simulation, the drying front remained stable until the air reaches the network bottom. That means, this in the simulation is almost not extended.

c)  $dT/dz = 0$

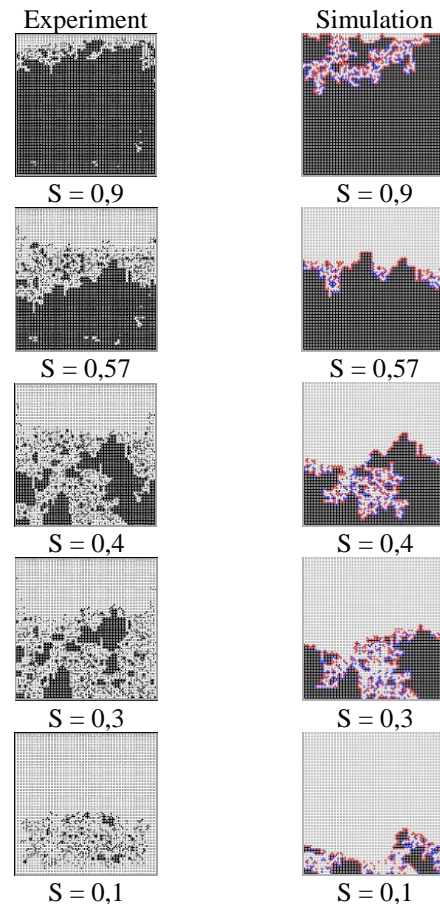


**Fig.9.** Phase distribution of the experiment and simulation for case  $T=63^\circ\text{C}$

In the isothermal drying, the phase distribution between the experiment and simulation do not reached the desired agreement (Fig. 9). In the first stage, the drying fronts of the both cases are relative stable. An early breakthrough is unobservable (to  $S = 0,57$ ). In experiments, many single clusters are separated from the drying front. But they still maintain their existence longer, while in the simulation these clusters evaporate quickly. This might be an evidence for the existence of liquid films in experiments. Breakthrough also be occurred earlier in experiment ( $S = 0,4$ ) than in the simulation ( $S = 0,3$ ). In the final stages, the liquid phase in both the experiment and the simulation locates deep in the bottom of the network.

#### 4. Conclusion

In this investigation the drying experiments on the pore network are conducted under isothermal and non-isothermal conditions. In the experiments effect of temperature on the drying process is investigated in 3 cases: constant temperature with  $T = 63^{\circ}\text{C}$ ; positive temperature gradient with  $T_0 = 27^{\circ}\text{C}$ ,  $T_L = 50^{\circ}\text{C}$ ; and negative temperature gradient with  $T_0 = 75^{\circ}\text{C}$ ,  $T_L = 53^{\circ}\text{C}$ . The temperature distribution on the network affects the phase distribution mainly and thus impacts the drying rate. The temperature has impact on surface tension, saturation vapor pressure and diffusion coefficient. When temperature increases, the surface tension decreases and that leads to increase of liquid pressure. From that, an application of temperature gradient on the network can affect the order of emptying of the pores. A negative temperature gradient ( $T_0 > T_L$ ) leads to a flat drying front, homogenous and stable. It can be explained that in this case the drying front always continuously moves away from the network opened side, the high drying rate in the beginning will drop quickly and then is maintained at low levels. By contrast, a positive temperature gradient ( $T_0 < T_L$ ) causes a branching and a stretched drying front, with the separation of many small clusters (unstable drying front). In this case, condensation appears leading to the creation of new clusters. High drying rate is maintained because the full pores at the network open continuously draws water from the network inside. In the case of isothermal drying, the drying front in the beginning is relative stable. Then, the width of the drying front gradually increases and the main cluster is divided into many small clusters, which exist for a long time in the network and maybe crease liquid films.

The simulation results show that the behavior of the simulated drying process is matched with the behavior observed in experiments. Especially, the phase distribution in experiments and simulations are

quire similar. However, though the drying rates are also located on the same magnitude and the drying curves have the same shape of qualitative, but they are quantitatively different (drying time difference has approximately the factor of 2). The cause of this may be due to the neglect of liquid films in the simulations. The liquid films in experiment can transport water to the network open and then lead to the increase of drying rate.

#### Notation

$dT$	Temperature gradient
$z$	Axis from the network opened side in the direction to the network bottom
$T_0$	Temperature at the network opened side
$T_L$	Temperature at the network bottom

#### References

- [1] V.K. Surasani, T. Metzger, E. Tsotsas, Influence of heating mode on drying behavior of capillary porous media: Pore scale modeling, *Chemical Engineering Science* 63, (2008)5218-5228.
- [2] A.G. Yiotis, I. N. Tsimpanogianis and A.K. Stubos, Fractal characteristics and scaling of the drying front in porous media: A pore network study, *Drying Technology*, 28: 8, (2010) 981 – 990.
- [3] J. B. Laurindo, M. Prat, Numerical and experimental network study of evaporation in capillary porous media – Drying rates, *Chemical Engineering Science* Vol. 53, No. 12, (1998) 2257-2269.
- [4] J. B. Laurindo, M. Prat, Numerical and experimental network study of evaporation in capillary porous media – Phase Distribution, *Chemical Engineering Science* Vol. 51, No. 23, (1996) 5171-5185.
- [5] F. Plourde, M. Prat, Pore network simulations of drying of capillary porous media. Influence of thermal gradients, *International Journal of Heat and Mass Transfer* 46, (2003) 1293-1307.
- [6] H.P. Huinink, L.Pel, M.A.J. Michels, M. Prat, Drying processes in the presence of temperature gradients – Pore-scale modeling, *Chemical Engineering Science* Vol. 51, No. 23, (2002) 5171-5185.
- [7] V.K. Surasani, T. Metzger, E. Tsotsas, 2008, Consideration of heat transfer in pore network modeling of convective drying, *International Journal of Heat and Mass Transfer* 51, (2002) 2506-2518.
- [8] M. Prat, Isothermal drying of non-hygroscopic capillary-porous materials as an invasion percolation process, *Int. J. Multiphase Flow* Vol. 21, No. 5, (1995) pp. 875-892.